Experimental Study on Influence of Unloading Rate on Creep Characteristics of Marble under High Stress

Huajun He[1] and Huahui Jin[1*]

[1]Zhejiang Guangchuan Engineering Consulting Co, Hangzhou 310020, China

Abstract. In the engineering of high stress area, the measures to control the stability of surrounding rock by reducing excavation footage and excavation speed are to adjust the unloading rate of surrounding rock caused by excavation. In this study, unloading creep tests of marble under high stress conditions were carried out to study the effect of unloading rate. Research results showed that the axial and lateral instantaneous strain and creep strain of the sample increased with the increase of unloading rate; the lateral creep characteristic of marble under unloading condition was stronger than that of axial creep characteristic, and it was more obvious with the increase of unloading rate; the failure of specimens under unloading creep condition was mainly caused by the rapid increase of lateral strain, and the brittleness of rock was increasing with the increase of unloading rate. The Burgers model was used to describe the creep curves of specimens, and the variation of the parameters with the unloading rate was analyzed. The fitting results showed that the instantaneous elastic modulus E_1, E'_1 and the viscosity coefficients η_1, η'_1 all decreased with the increase of the unloading rate, which can be described by linear relationship within the unloading rate range of this experiment. Compared with the time of whole creep tests, the time for each specimen to enter the steady-state creep was similar, it was considered that the effect of unloading rate on η_2/E_2 and η'_2/E'_2 can be ignored.

1 Introduction

Compared to the soft rock material, it is generally considered that the hard rock material has relatively weak viscosity[1,2]. With the continuous construction of some large-scale projects, more and more practice shows that in the process of excavation or unloading of valley trenching under high ground stress, in addition to the common surface rock mass failure (such as rockburst) in a short time due to the rapid release of elastic strain energy, the deformation and failure of hard rock generally have to go through a more obvious time-dependent process. The above phenomenon are strongly manifested in hard rock projects such as granite in the Three Gorges Hydropower Project[3], marble in the Jinping Hydropower Station[4], sandy slate in the river reaches of the Yalong River Hydrological Station[5], and granite in the reservoir area of the Laxiwa Hydropower Project in the upper reaches of the Yellow River[6]. In view of this, many scholars have been conducted studies on the creep characteristics of hard rock under unloading by using experiments and related theories. Such as Yan[7] carried out unloading creep tests with lateral stress unloading gradually on the marble of the Jinping Hydropower Station diversion tunnel, and pointed out that there were significant differences between the axial and lateral deformation. Zhu[8] carried out triaxial unloading creep tests on the green sandstone of the Jinping II Hydropower Station, and established the rock damage evolution equation and variable parameter nonlinear Burgers model. Yang[9] prepared fractured specimens from Chongqing sandstone, carried out triaxial unloading creep tests and proposed a damage creep model to establish the relationship between intact rock and fractured rock mass.

Based on the analysis of current studies, the differences of creep properties of hard rock have been investigated from different unloading values[10], different loading-unloading paths[11], different initial confining pressure and other conditions, while the researches on creep characteristics of hard rock under different unloading rates are relatively less. Moreover, the relevant research results of conventional unloading tests of hard rock show that the unloading rate has a significant impact on mechanical properties. In fact, the essence of the measures to control the stability of the surrounding rock by reducing the excavation footstep and lowering the excavation speed in practical projects in high stress areas is to adjust the unloading rate of the surrounding rock caused by excavation[11].

In this study, the unloading creep tests of hard marble under high initial confining pressure were carried out, the effects of different unloading rates on the deformation, strength and failure mode of the materials were investigated, and a creep model considering the effects of different unloading rates was established. The results can provide references for the unloading creep characteristics of hard rock and the evaluation of the time-dependent stability of hard rock projects in high stress areas.

* Corresponding author: 691436049@qq.com

2 Testing procedure

The Specimens made from marble had a columnar shape witch a diameter of 50 mm and a height of 100 mm, which were accordance with the standard recommended by the International Society for Rock Mechanics. The specimens were taken from the same rock mass with dry densities of 2.62-2.81 g/cm^3 and the peak strength σ_c of about 128.5 MPa at the confining pressure σ_3=0.6 MPa. In order to ensure the failure of specimens during tests, the initial axial compression σ_1 and initial high confining pressure σ_3 were set to 130 MPa and 40 MPa, respectively. In the test process, the axial compression σ_1 was constant and the confining pressure σ_3 was unloaded gradually, the unloading value $\Delta\sigma_3$ was constant (15 MPa) and the unloading rate $v_{\Delta\sigma3}$ was 0.10 MPa/s, 0.3 MPa/s, 0.6 MPa/s and 0.9 MPa/s, respectively. Firstly, the confining pressure σ_3 was loaded at a rate of 0.05 MPa/s, and the axial compression σ_1 was loaded at a rate of 0.5 kN/s up to 40 MPa. Secondly, σ_1 was loaded at a rate of 0.5 kN/s up to 130 MPa. Thirdly, the σ_1 and σ_3 were kept constant until the creep deformation of specimens stabilized (the observed displacement increment must be less than 0.001 mm/h[12], and the time must not be less than 50 h). Finally, the σ_1 was kept constant, while the σ_3 was unloaded with the set unloading rate $v_{\Delta\sigma3}$ to the set value. After the deformation of specimens under each level of confining pressure reached stability, then the next level of unloading was carried out until the tests ended when specimens were destroyed.

3 Results

The creep curves of specimens obtained in creep tests under different unloading rates are plotted in Fig. 1. The ranges of axial and lateral instantaneous strain of the four specimens loaded to the initial stress state (σ_1=130MPa, σ_3=40MPa) were 0.415%–0.421% and 0.074%–0.080%, and the ranges of axial and lateral creep strains were 0.082%–0.092% and 0.022%–0.036%, respectively, which indicated that the dispersion of specimens was well controlled.

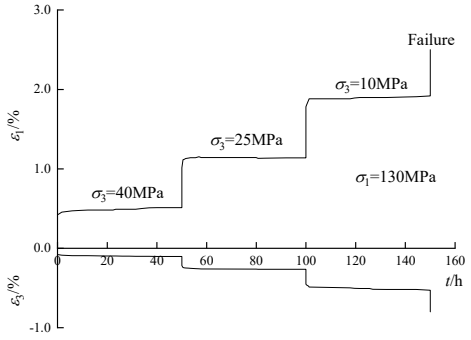

(a) 0.1 MPa/s

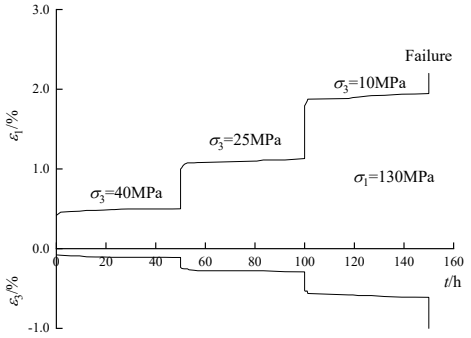

(b) 0.3 MPa/s

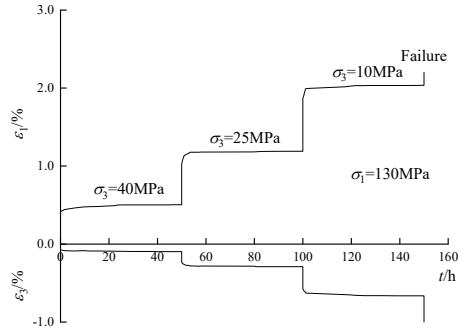

(c) 0.6 MPa/s

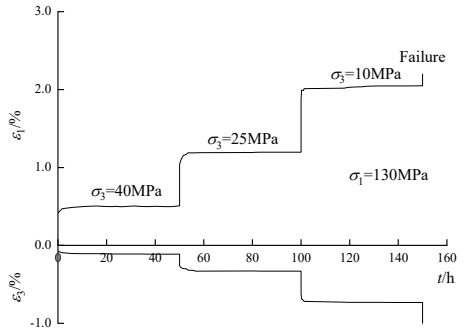

(d) 0.9 MPa/s

Fig. 1. Curves of specimens obtained in creep tests under different unloading rates

Table 1 summaries the instantaneous strain and creep strain of specimens under different unloading rates. It can be observed that with the increase of unloading rate, the instantaneous strain and creep strain of all axial and lateral increased, but the increase of lateral was larger than that of axial. Taking the instantaneous strain and creep strain of specimens at the unloading rate $v_{\Delta\sigma3}$=0.1 MPa/s as an example, when the stress level σ_3=25 MPa, for $v_{\Delta\sigma3}$=0.3, 0.6 and 0.9 MPa/s, the percent increase of axial instantaneous strain for specimens were -0.5%, 4.7% and 6.4%, while that of lateral instantaneous strain were 9.4%, 17.1% and 30.6%, respectively; the percent increase of axial creep strain for specimens were 6.1%, 28.9% and 24.0%, while that of lateral creep strain were 18.4%, 25.2% and 44.2%, respectively. When σ_3=10 MPa, for $v_{\Delta\sigma3}$=0.3, 0.6 and 0.9 MPa/s, the percent increase of axial instantaneous strain for specimens were 3.1%, 5.5% and 5.7%, while that of lateral instantaneous strain were 24.8%, 49.6% and 55.5%, respectively; the percent increase of axial creep strain for specimens were 10.5%,

20.9% and 25.8%, while that of lateral creep strain were 12.1%, 21.1% and 46.1%, respectively.

Table 1. Instantaneous strain and creep strain of specimens under different unloading rates (σ_1=130 MPa)

σ_3 / MPa	$v_{\Delta\sigma 3}$ / (MPa/s)	axial		lateral	
		ε_0/ %	ε_i/ %	ε_0/ %	ε_i/ %
25	0.5008	0.1253	-0.1149	0.0468	0.5008
	0.4980	0.1330	-0.1257	0.0554	0.4980
	0.5245	0.1615	-0.1346	0.0585	0.5245
	0.5326	0.1554	-0.1501	0.0674	0.5326
10	0.6433	0.1368	-0.1874	0.0772	0.6433
	0.6633	0.1511	-0.2337	0.0866	0.6633
	0.6788	0.1654	-0.2803	0.0935	0.6788
	0.6801	0.1721	-0.2913	0.1128	0.6801

It also can be indicated from the above data that the increase of stress differences (σ_1-σ_3) affected the increase of lateral instantaneous strain and creep strain with $v_{\Delta\sigma 3}$. The variation curves of the ratio of lateral strain ε_3 to axial strain ε_1 ($\mu = \varepsilon_3 / \varepsilon_1$) with $v_{\Delta\sigma 3}$ of specimens at the initial moment and the end time of creep at different stress levels are shown in Fig. 2. The curves showed an upward trend in all four states, that is, μ increased with $v_{\Delta\sigma 3}$. It was obvious that the increasing slope of the two curves at σ_3=25 MPa was slower than that at σ_3=10 MPa, which indicated that the increasing trend of μ with $v_{\Delta\sigma 3}$ was stronger at σ_3=10 MPa. When $v_{\Delta\sigma 3}$ was constant, μ would increase with the creep time, and the increase of μ would occur at the moment of unloading the next level of the confining pressure. A larger number of experimental results[13] show that the axial and lateral creep deformation of marble under unloading conditions are significantly different, and the lateral creep characteristics are more obvious than the axial characteristics. This point was not only verified by the test results in this study, but also more obvious with the increase of unloading rates.

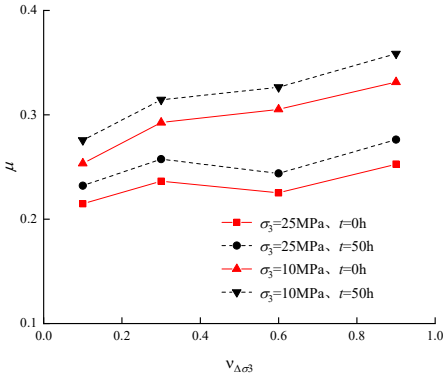

Fig. 2. Relationship between μ and $v_{\Delta\sigma 3}$

The failure of all four specimens occurred during the third stage of unloading, and the images of failure are shown in Fig. 3. All specimens showed the failure characteristic of macroscopic shear surface, while the angle of the rupture surface increased with the unloading rate. For $v_{\Delta\sigma 3}$=0.1, 0.3, 0.6 and 0.9 MPa/s, the angle of the rupture surface were about 60°, 62°, 67° and 71°, respectively. By combining the data in Table 1 and Fig. 2, it can be concluded that the failure of specimens under unloading creep conditions was mainly due to the rapid increase of lateral strain. Moreover, the brittleness of specimens was increasing as the unloading rate increased.

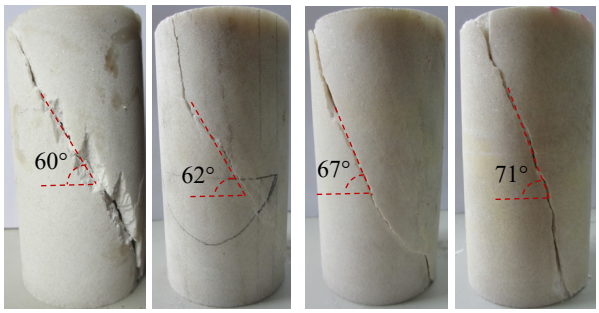

(a) 0.1 MPa/s (b) 0.3 MPa/s (c) 0.6 MPa/s (d) 0.9 MPa/s

Fig.3. Failure of specimens under different unloading rates

4 A modified Burgers model

4.1. The Burgers model and parameter inversion

Since specimens were all failed during the unloading process, the creep curves of each specimen were fitted with the conventional element model, which aimed to investigate the effect of unloading rates on the parameters of the element model.

After dealing with the specimen creep curves by Chen method, it was found that the Burgers model had a good fitting effect on each curve. The Burgers model is shown in Fig.4, which can be described under three-dimensional stress state as

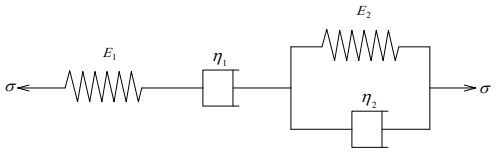

Fig. 4. Burgers model

$$e_{ij} = \frac{S_{ij}}{2G_1} + \frac{S_{ij}}{2G_2}\left[1 - e^{-\frac{G_2}{\eta_2}t}\right] + \frac{S_{ij}}{2\eta_1}t \quad (1)$$

$$\varepsilon_m = \frac{\sigma_m}{3K} \quad (2)$$

where e_{ij} is the deviatoric strain; S_{ij} is the deviatoric stress; K is the bulk modulus; G_1 and G_2 are the shear modulus; ε_m is the spherical strain; σ_m is the spherical stress; K, G_1, G_2, η_1 and η_2 are the mode parameters, which are determined by fitting the test results. E_1 and E_2 in Fig. 4 can be transformed into K, G_1 and G_2 by the equation of elastic mechanics. The creep curves of each specimen were fitted by Eqs. (1) and (2), and the creep parameters under different conditions were obtained as shown in Table 2.

Table 2. Parameters of Burgers model

Stress levels		$v_{\Delta\sigma 3}$ / (MPa/s)	Axial parameters			
σ_1 /MPa	σ_3 /MPa		E_1 /MPa	η_1 /MPa·h	E_2 /MPa	η_2 /MPa·h
130	25	0.1	23680	8081367	13332	9931
		0.3	20088	7643015	13930	9544
		0.6	22021	7225685	12944	9332
		0.9	21060	6119210	12879	10354
	10	0.1	14051	4272541	9923	10313
		0.3	13483	3951055	9041	9861
		0.6	13437	3815453	8994	7926
		0.9	9717	3986541	7250	9432
			Lateral parameters of the Burgers model			
			E'_1 /MPa	η'_1 /MPa·h	E'_2 /MPa	η'_2 /MPa·h
	25	0.1	90053	6616545	43321	34601
		0.3	83099	5835348	43161	45534
		0.6	84482	5550801	38898	41557
		0.9	74308	5436124	33978	49713
	10	0.1	38071	3560884	21659	39212
		0.3	32768	2606195	19279	35671
		0.6	30147	2604686	20283	33692
		0.9	23830	1747717	58371	54510

4.2 The effect of the unloading rate on the parameters

For the Burgers model, the instantaneous elastic modulus E_1 and E'_1 reflect the instantaneous deformation of specimens; the viscosity coefficients η_1 and η'_1 reflect the rate of the steady-state creep stage; η_2/E_2 and η'_2/E'_2 reflect the time to reach the steady-state creep stage. Fig. 5 shows the variation curves of E_1, E'_1, η_1 and η'_1 with the unloading rate $v_{\Delta\sigma 3}$, from which several conclusions can be drawn as followings:

(1) For E_1 and E'_1, which basically decreased as $v_{\Delta\sigma 3}$ increased, the relationship can be expressed by linear function fitting within the unloading rate ranges of this experiment as

$$\text{When } \sigma_3\text{=25MPa, } \begin{cases} E_1 = -1.88v_{\Delta\sigma 3} + 22.61 \\ E_1^{'} = -16.79v_{\Delta\sigma 3} + 90.96 \end{cases} \quad (3)$$

$$\text{When } \sigma_3\text{=10MPa, } \begin{cases} E_1 = -4.95v_{\Delta\sigma 3} + 15.02 \\ E_1^{'} = -16.64v_{\Delta\sigma 3} + 39.91 \end{cases} \quad (4)$$

It can be seen that the decreasing rate of the lateral elastic coefficient E'_1 was greater than that of the axial elastic coefficient E_1. Under different stress levels, the fitting lines of axial and axial, radial and radial were almost parallel at different stress levels. That is, the creep characteristics were less affected by the stress levels compared to the axial and lateral ones.

(2) For η_1 and η'_1, which basically decreased as $v_{\Delta\sigma 3}$ increased, the relationship can also be expressed by linear function fitting within the unloading rate ranges of this experiment as

$$\text{When } \sigma_3\text{=25MPa, } \begin{cases} \eta_1 = -2351.5v_{\Delta\sigma 3} + 8384.3 \\ \eta_1^{'} = -1355.6v_{\Delta\sigma 3} + 6503.5 \end{cases} \quad (5)$$

$$\text{When } \sigma_3\text{=10MPa, } \begin{cases} \eta_1 = -335.5v_{\Delta\sigma 3} + 4165.0 \\ \eta_1^{'} = -1967.5v_{\Delta\sigma 3} + 3564.4 \end{cases} \quad (6)$$

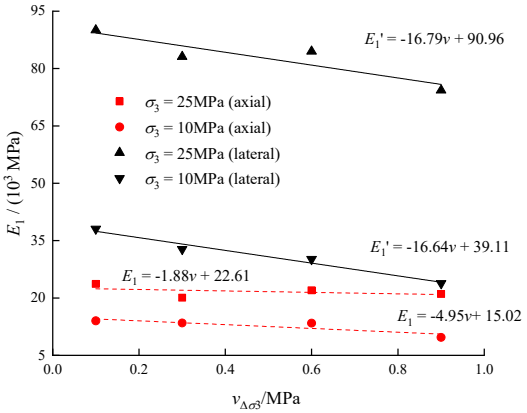

(a) the instantaneous elastic modulus E_1

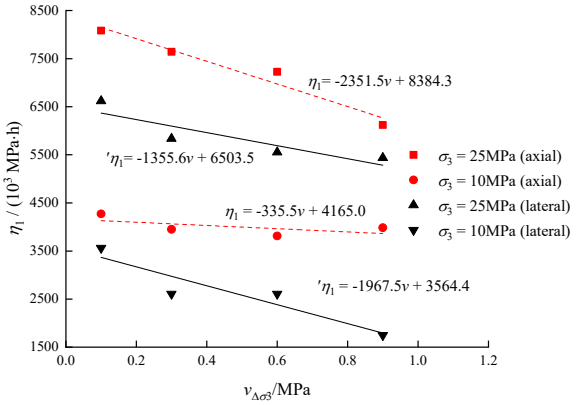

(b) the viscosity coefficients η_1

Fig. 5. Model parameters change with unloading values

(3) The law of variation of E_2, E'_2, η_2 and η'_2 with $v_{\Delta\sigma 3}$ was not obvious. According to the physical meaning of the Burgers model, the minimum and maximum values of η_2/E_2 were 0.685 h and 1.301 h, while the minimum and maximum values of η'_2/E'_2 were 0.799 h and 1.850 h, respectively. Compared with the time of the entire creep process (each load stage of 50 h), the time of each specimen entering the steady-state creep stage was similar. So it was considered that the effect of $v_{\Delta\sigma 3}$ on η_2/E_2 and η'_2/E'_2 can be neglected in this study.

Based on the above analysis, the creep model for marble considering the effect of unloading rate can be obtained by substituting Eqs. (3)–(6) into Eqs. (1)–(2).

5 Conclusions

The stress of rock is unloading during the excavation of deep buried tunnel, it is necessary to study the creep behavior of rock under unloading condition.In order to analyze the influence of unloading rate on the unloading creep of hard rock, the triaxial unloading creep tests under high stress were carried out on marble in this study, and a modified Burgers model considering the influence of unloading rate was established based on the test results. The results showed that the unloading rate had a significant effect on the unloading creep characteristics of marble, the conclusions can be generally summarized as:

(1) With the increase of unloading rate, all instantaneous strain and creep strain of axial and lateral increased, while the increase of lateral was significant larger than that of axial.

(2) With the increase of unloading rate, the angle of the rupture surface increased. It can be inferred that the failure of specimens under unloading creep condition was mainly due to the rapid increase of lateral strain. Moreover, with the increase of unloading rate, the brittleness of rock was increasing.

(3) E_1, E'_1, η_1 and η'_1 decreased as $v_{\Delta\sigma 3}$ increased, the relationship of which can be fitted by linear function. The fitting results showed that the decreasing rate of the lateral elastic coefficient E'_1 was greater than that of the axial elastic coefficient E_1, and the fitting lines of axial and axial, lateral and lateral were basically parallel under different stress levels.

(4) The difference between the minimum value and the maximum value of η_2/E_2 and η'_2/E'_2 was small. Compared with the creep time of the whole test (each load stage of 50 h), the time of each specimen entering the steady-state creep stage was similar. Therefore, the effect of $v_{\Delta\sigma 3}$ on η_2/E_2 and η'_2/E'_2 can be neglected in this study.

(5) The further research will be carried out from the numerical calculation of the model established in this paper, so as to realize the engineering application.

References

1. WANG Junbao, LIU Xinrong, SONG Zhanping. A whole process creeping model of salt rock under uniaxial compression based on inverse S function. Chinese Journal of Rock Mechanics and Engineering, 2018, 37(**11**): 2446 - 2459.
2. YANG Chao, HUANG Da, CAI Rui. Triaxial unloading creep test of open-through single-fracture rock mass. Geotechnical Mechanics, 2018(**1**): 53 – 62.
3. CHEN Deji, YU Yongzhi, MA Nengwu. Some main problems on the stability of high permanent shiplock slope for three gorges project. Journal of Engineering Geology, 2000, 8(**1**): 7 – 15.
4. HUANG Runqiu, HUANG Da, DUAN Shaohui. Geomechanics mechanism and characteristics of surrounding rock mass deformation failure in construction phase for underground powerhouse of jinping I hydropower station. 2011, 30(**1**): 23 – 35.
5. WANG Shitian, HUANG Runqiu, LI Yusheng. Research on major engineering geological problems of Jinping hydropower station on Yalong river. Chengdu: Chengdu University of Science and Technology Press, 1995.
6. HUANG Runqiu, ZHANG Zhuoyuan, WANG Shitian. Systematic engineering geology research on high slope stability. Chengdu: Chengdu University of Science and Technology Press, 1991.
7. YAN Zijian, XIA Caichu, LI Hongzhe. Study on rheological rules of marble in Jinping hydropower station under condition of step unloading. Chinese Journal of Rock Mechanics and Engineering, 2008, 27(**10**): 2153 – 2159.
8. ZHU Jiebing, WANG Bin, WU Aiqing. Study of unloading triaxial rheological tests and its nonlinear damage constitutive model of Jinping hydropower station green sandstone. Chinese Journal of Rock Mechanics and Engineering, 2010, 29(**3**): 528 – 534.
9. YANG Chao, HUANG Da, HUANG Runqiu, Zeng Bin. Experimental study on the triaxial unloading creep characteristics of stone with two pre-existing cracks and its damage creep model. The Journal of Coal, 2016, 41(**9**): 2203 – 2211.
10. HUANG Da, YANG Chao, HUANG Runqiu, Liu Jie. Experimental restarch of unloading triaxial rheological characteristics of marble affected by different step unloading values. Journal of Rock Mechanics and Geotechnical Engineering, 2015(**S1**): 2801 - 2807

11. JIANG Yuzhou, WANG Ruihong, Zhu Jiebing. Experimental study of creep and elastic after-effects properties of sandstone. Journal of Rock Mechanics and Geotechnical Engineering, 2015, 34(**10**): 2010 – 2017.
12. DING Yanzhi, ZHANG Qiangyong, Zhang Longyun. Three axis creep test and analysis of granite in underground laboratory of deep geological disposal. Journal of Central South University (Natural Science Edition), 2019, 50(**4**): 957 – 967.
13. QIU Shili, FENG Xiating, ZHANG Chuanqing. Experimental restarch on mechanical properties of deep-buried marble under different unloading rates of confining pressures. Joumal of Rock Mechanics and Geotechnical Engineering, 2010, 29(**9**): 1807 – 1817.
14. SUN Jun. Geotechnical material rheology and its engineering application. Bei jing: China Architecture & Building Press, 1999: 411 – 412.